Semicond. Sci. Technol. **23** (2008) 075040 (6pp) doi:10.1088/0268-1242/23/7/075040

Gold-enhanced oxidation of MBE-grown silicon nanowires

C C Büttner, N D Zakharov, E Pippel, U Gösele and P Werner

MPI of Microstructure Physics, Weinberg 2, D-06120 Halle (Saale), Germany

Received 13 February 2008, in final form 10 April 2008
Published 28 May 2008
Online at stacks.iop.org/SST/23/075040

Abstract

Thermal oxidation of MBE-grown silicon nanowires with a gold droplet on their tips was investigated. Two kinds of oxidation behavior were observed: (i) *enhanced axial oxidation*, if there was a direct contact between the gold droplet and the nanowire, and (ii) *conventional oxidation* for nanowires when there was no direct contact between the gold and silicon. For a dry atmosphere, such enhanced oxidation takes place at temperatures down to 500 °C. Under a wet atmosphere, remarkable oxidation was observed even for temperatures down to 250 °C.

1. Introduction

Silicon nanowires (Si NWs) are of great interest for microelectronic applications due to their unique electrical and optical properties. Very thin semiconductor NWs with a diameter of about 5 nm show physically interesting quantum confinement effects [1]. Thicker NWs can be thinned down via thermal oxidation [2–4] in order to achieve quantum confinement effects. However, electrically active defects on the NW surface, the so-called surface states, can also be reduced by an oxidation procedure.

Thermal oxidation of Si, in general, takes place according to the Deal–Grove model [5]. In the present paper, it is denoted as 'conventional oxidation'. The oxidizing agent diffuses through an already existing oxidized layer and oxidizes the silicon at the interface Si/SiO_2. Thereby, the oxide layer already formed is being pushed outwards. At the beginning, the oxidation reaction has a linear behavior because the oxidation is reaction controlled. With increasing oxide thickness, the oxidation rate changes to a parabolic behavior since the reaction gets more and more diffusion controlled. For the very initial oxidation regime the oxidation rate is much faster, which was explained by Massoud and Plummer [6]. For cylindrical structures, some changes occur additionally because in this case the oxidation is retarded due to the occurrence of stresses [3, 7, 8].

The results of the reaction of a cylindrical, one-dimensional structure should be compared with the studies on oxidation experiments on Si wafer surfaces covered by a thin Au film. Corresponding experiments on such two-dimensional structures have been intensively carried out during the last 30 years [9–12], yielding different reaction models. All of these models discuss the possibility that the bonds of a Si lattice are weakened when they are in contact with Au. Thereby the Si atoms, which are lying at the Si/Au layer interface, can easily diffuse into and through the gold. They are oxidized at the surface of the two-dimensional Au layer in an oxidizing atmosphere [9]. It was observed that the oxidation proceeds at a much higher oxidation rate and at lower temperatures than the conventional oxidation of bulk Si.

For a discussion of the oxidation behavior of NWs, the specific conditions of their formation have to be taken into account. Semiconductor NWs are quite often grown by the so-called vapor–liquid–solid mechanism (VLS) (see, e.g., [13]). It is characterized by small metal droplets, which act as catalytic particles for the NW synthesis. The metal droplets (often gold is used) are on the tip of the growing NW; there is always a direct contact between the droplet and the generated semiconductor crystal lattice. In the present paper, we have investigated the oxidation behavior of NWs grown by molecular-beam epitaxy (MBE). In this case, the growth mechanism differs from the classical VLS [14, 15]. When these Au-capped NWs are oxidized, enhanced axial oxidation can occur. This phenomenon was already experimentally observed by Westwater *et al* [16] in 1997, but not further discussed at that time. This gave us the motivation for a more detailed experimental study of this phenomenon of the enhanced oxidation reaction on Si NWs. The first preliminary results were reported in [17]. Here we present a more detailed analysis.

2. Experiment

Undoped single-crystalline ⟨1 1 1⟩ Si NWs were grown in a MBE chamber at a temperature of 525 °C and at a pressure

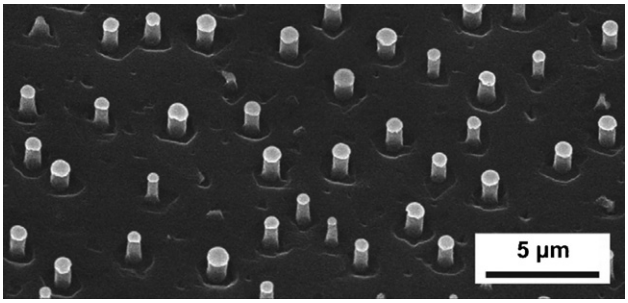

Figure 1. An inclined SEM image of MBE-grown Si NWs before oxidation. On their tips are hemispherical Au:Si eutectic droplets [15]. NWs are surrounded by trenches where the material is consumed due to Si diffusion.

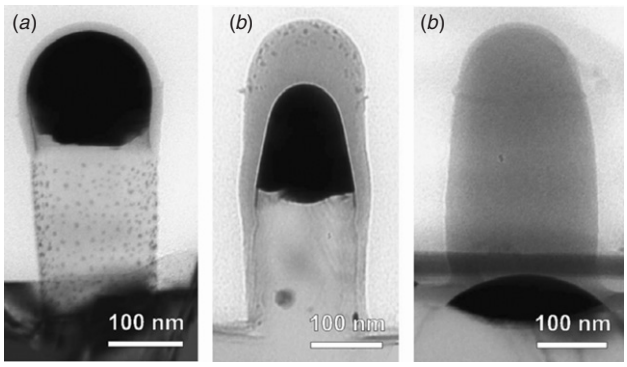

Figure 2. TEM images for the temperature-dependent oxidation behavior for dry oxidation at a constant time of 3 h for different temperatures: (*a*) 500 °C, (*b*) 750 °C, (*c*) 850 °C.

of 10^{-9} mbar [14, 18]. First, Au is evaporated onto a ⟨1 1 1⟩ oriented Si substrate with a nominal thickness of 2 nm. Because of the high temperature, droplets are formed that have a diameter distribution which can be described by an Ostwald ripening process. The mean diameter amounts to about 110 nm. Furthermore, the droplets are transformed into an Au:Si alloy (eutectic temperature for Au–Si: 360 °C; see, e.g., [19]). It has to be mentioned that beside the droplets, a Au-wetting layer is formed on the whole substrate consisting of a Si–Au eutectic phase and having a thickness of a few monolayers [15]. In the next step, Si is evaporated using an e-beam evaporator. The Au droplets consume the Si adatoms from the surrounding, and the NW growth proceeds from the Au/Si eutectic supersaturated by Si [15]. MBE-grown Si NWs are characterized by a low aspect ratio with diameters between 80 and 160 nm and lengths between 100 and 500 nm. An example of the NWs is presented in figure 1.

Thermal oxidation experiments were carried out both in dry and in wet atmospheres. First results were reported by the authors in [17]. Dry oxidation was carried out in a tube zone furnace at temperatures between 250 °C and 1000 °C, using a constant gas flow of 70 SCCM (cubic centimeter per minute at STP) nitrogen and 30 SCCM oxygen. This composition was chosen to simulate a reaction under normal ambient air. At the beginning, the furnace was pumped down followed by the heating up under a N_2 atmosphere to avoid any pre-oxidation. After reaching the desired oxidation temperature, the gas was switched to a mixture of oxygen and nitrogen. To stop the reaction, the gas flow was immediately switched back to N_2 and the furnace was cooled down.

Wet oxidation was carried out in two different systems. Most of the experiments were performed in a furnace using normal air, which included ambient humidity. Even though the humidity might have slightly changed within such oxidation series, the results received were qualitatively comparable. As a reference experiment, the wet oxidation was realized in a tube furnace with an unheated bubbler. The nitrogen gas stream was guided through a water vessel and thereby saturated with water molecules. The wet oxidation was done at 100 °C and 250 °C for oxidation times of 5 min, 10 min, 15 min, 30 min, 1 h, 3 h and 6 h, respectively.

The morphology of the NW samples was analyzed by TEM and scanning TEM (STEM). The chemical composition was identified by electron energy-loss spectroscopy (EELS) available in the STEM (accelerating voltage 200 kV, STEM point resolution 0.5 nm, energy resolution 0.6 eV).

3. Results and discussion

In principle, two different kinds of oxidation behavior of Si NWs were observed, as described in the following: (i) conventional oxidation and (ii) enhanced axial oxidation of the NWs. The characteristic feature for the latter case was an increased reaction of freshly grown NWs in the axial direction. At the sidewalls of the NWs, however, a formation of oxide layers was observed with a growth rate expected from conventional oxidation. Furthermore, (iii) in comparison to oxidation at a dry atmosphere, the NWs can be oxidized at much lower reaction temperatures, when a wet atmosphere is applied. Therefore, the results are divided into three subsections.

3.1. Enhanced axial oxidation under a dry atmosphere

Figure 2 presents TEM cross-section images of dry-oxidized Si NWs at different reaction temperatures for a reaction time of 3 h. The dark regions correlate to the Au:Si eutectic cap promoting the fast reaction. Note that the gray spots (size <5 nm) on the NW surface, especially visible in figure 2(*a*), are Au-containing clusters and are the result of the VLS-growth process of the Si NWs. When cooling down the wafer, the Au wetting layer mentioned on the surface collapses, forming small clusters.

The NWs got shorter quite fast during oxidation and at the same time, a SiO_2 wire was formed on the top of the droplet. The mechanism of this reaction is schematically shown in figure 3. It can be assumed that the droplet consists of a Au:Si eutectic, since immediately after increasing the reaction temperature ($T > 360$ °C) Si atoms are dissolved from the NW into the droplet. This experimental behavior is similar to the enhanced oxidation of planar silicon covered by a gold layer

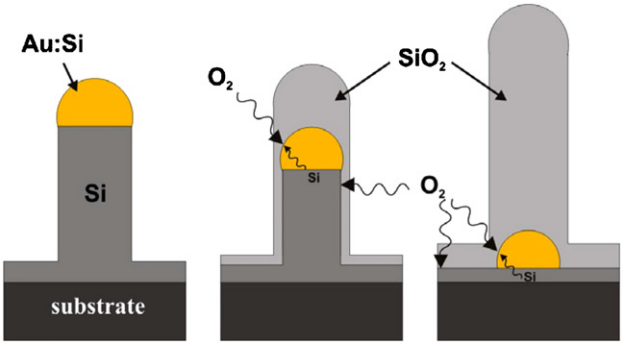

Figure 3. Schematic diagram of the enhanced oxidation of Si NWs. In this case, there is a direct contact between the Si NW and the Au:Si droplet (yellow).

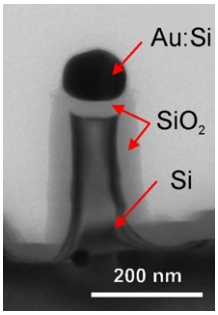

Figure 4. TEM image of a Si NW dry oxidized at 850 °C for 3 h. In this case, a SiO_2 film (gray) was formed before the thermal oxidation preventing the Si pillar from silicon diffusion through the Au droplet.

on top, observed by several different research groups [9–12]. These authors assumed that the covalent bonds of the Si atoms at the interface to the gold were weakened due to the presence of Au. Thereby single Si interface atoms will, as a first step, be fast removed from the crystal lattice and diffused into the liquid droplet. As a second step, the Si atoms diffuse through the gold and are oxidized on top of the Au:Si droplet. The SiO_2 pillar (light gray) generated by the reaction has a volume about twice as high as the Si NW. This relates to the different atomic volumes of Si (about 20 $Å^3$) compared to the SiO_2 volume (about 45 $Å^3$) [3].

3.2. Conventional oxidation under a dry atmosphere

In contrast to the above-mentioned behavior, no axial enhanced oxidation was observed in the case when the Au:Si droplet was not in a direct contact to the Si NW, but separated, e.g., by a thin amorphous oxide layer. Figure 4 presents a TEM image of a NW, which was oxidized at 850 °C in a dry atmosphere. Thereby, a SiO_2 layer was formed not only around the surface of the NW, but also between the Au:Si droplet and the Si pillar. In both cases, the thickness of the formed oxide corresponds nearly to the thickness of conventional oxidation described by the Deal–Grove model.

Even an intermediate SiO_2 layer of about 2 nm seems to suppress the enhanced reaction described above. Such thin layers have to be formed after the NW growth. We observed the occurrence of such amorphous layers by TEM in the case of wafer pieces, which were stored in air after the growth for 2–3 months before carrying out oxidation experiments. The nature of such thin amorphous layers was identified by EELS measurements as silicon oxide. An example of such an analysis is presented in figure 5. The chemical composition was determined along the red line.

The spectrum of the interface layer shows that it is a superposition of the spectra of Si and SiO_2. The characteristic peak at 101 eV belongs to Si and the one at 108 eV to SiO_2. Such thin oxide layers (thickness < 2 nm) might be the result of lateral oxidation of the Au/Si interface even at room temperature.

This thin oxide interface layer hinders the weakening of bonds of the Si lattice by the Au atoms. Therefore, enhanced oxidation can no longer occur because of this SiO_2 barrier layer, and the Si NWs oxidize in the conventional way. This mechanism is schematically shown in figure 6. The NW oxidizes equally from all sides.

It is of interest to compare the thickness of the oxide layer on such Si NWs with values of the two-dimensional layers formed on the wafer surface close to the NWs as well as with values of the predicted conventional oxide thickness. The results are demonstrated in figure 7 for two oxidation experiments at 750 °C and 850 °C, respectively. These experimental data were compared with the calculated ones for dry oxidation of planar ⟨1 1 1⟩ oriented silicon[1]. Corresponding graphs in figure 7 display the differences between dry oxidation at 750 °C (*a*) and 850 °C (*b*), respectively.

The experiments carried out at 750 °C demonstrate that the dry oxidation leads nearly to the same oxide thickness for the oxide shells around the Si NWs as well as for the planar Si wafer surface around them. This supports our assumption that the relative thick NWs behave as bulk material. An influence of their curvature, which might generate stress within the oxide shell observed for smaller NWs [3], seems to be negligible in the present case, where the oxide thicknesses are not larger than 20 nm. However, the experiments show that the experimentally measured oxide thicknesses are larger than the simulated ones (figure 7(*a*), black curve). The reason for this observation might be the following.The presence of Au-containing clusters, which results from the wetting layer for both the surfaces of the NWs (see figure 2(*a*)) and the planar Si surface, might be responsible for the slightly enhanced oxidation at 750 °C compared to the simulated values. The local oxide thickness above the gold clusters is thicker by a few nanometers which was confirmed with TEM measurements.

The observations for the case of dry oxidation at 850 °C slightly differ (figure 7(*b*)). Here, the experimental oxide thickness on the wafer surface correlates to the simulated thickness. However, the growth rate of the NW oxide decreases for shell thicknesses >30 nm. In this case, the

[1] The code was applied based on www.lelanstanfordjunior.com/thermaloxide.html.

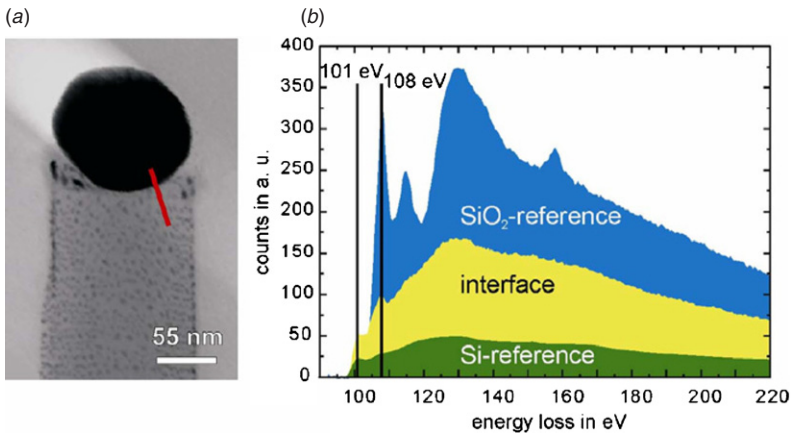

Figure 5. EELS measurement for the verification of a thin silicon dioxide layer between the Au:Si droplet and the Si NW. (*a*) The TEM picture of the analyzed NW, red: EELS linescan, (*b*) the EELS spectrum of the interface layer (yellow) contains the characteristic peak (108 eV) for SiO_2. Furthermore, reference spectra for crystalline Si (green) and SiO_2 (blue) are included.

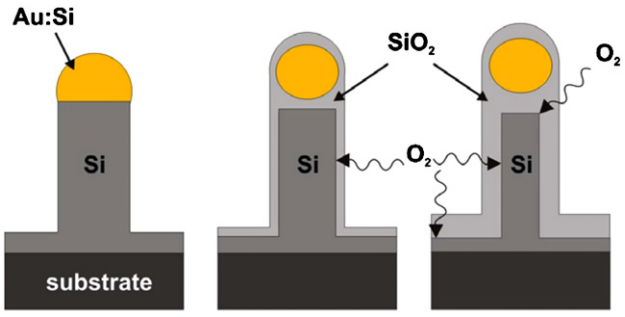

Figure 6. Schematic diagram of the thermal oxidation without direct contact between the Au:Si droplet and a Si NW (conventional oxidation—no enhanced axial oxidation occurs).

curvature of the thinner NW has to be taken into account. The developing mechanical stress within the SiO_2 shell increases drastically, thereby retarding the oxidation reaction [3, 4].

3.3. Si NW oxidation in a wet atmosphere

In the following, the results of dry oxidation will be compared with the experiments of the wet oxidation of NWs. In general, there are significant differences between both methods. This concerns, firstly, the experimental parameters. Water vapor has a much higher solubility in silicon dioxide (3×10^{19} molecules cm^{-3} at 1000 °C and ambient pressure) than oxygen (5.2×10^{14} molecules cm^{-3}). Additionally, the SiO_2 network gets more porous during wet oxidation because of the hydroxyl groups that are built into it. The smaller water molecules compared to oxygen molecules can diffuse quite fast in this porous network [20]. The gold-enhanced wet oxidation was also investigated for CVD-grown NWs by Xie *et al* [21].

Second, Si NWs oxidize much faster when using wet oxidation even at a low temperature. While for dry oxidation, an oxidation temperature of at least 850 °C and a reaction time of 6 h are needed to transform a Si NW completely into a NW of SiO_2, the same can be achieved by wet oxidation within 30 min at 250 °C (which is below the eutectic temperature of 360 °C).

Third, the morphology of the wet-oxidized NWs shows differences to that for dry-oxidized NWs. In the latter case, the NWs oxidize from the top to the base and the thereby generated SiO_2 wires are still perpendicular to the substrate. In the case of wet oxidation, a bent SiO_2 wire with a lamella-like oxide structure is formed. Figure 8 shows the different morphologies for a dry oxidized NW in comparison to a wet oxidized NW. It has to be mentioned that the actual temperature at the NW reaction interface might be higher in comparison to the measured furnace temperature due to the heat generated during oxidation.

Wet-oxidized Si NWs are characterized by lamella-like morphology, where the oxide has a segmented structure. Xie *et al* [21] found a similar behavior in the case of oxidized Si NWs grown by LP-CVD. We assume that the rapid oxidation reaction might cause such morphology. The generated oxide is pushed out after a certain thickness because of the existing stress. Due to the instability, the whole oxide layer is lifted and a new SiO_2 layer is formed, which is still connected to the old one. This mechanism explains the lamella-like structure.

It is striking that for wet-oxidized NWs, the Au:Si droplets are often elongated and separated into smaller droplets. This also happens for dry oxidation but mostly at higher temperatures and for longer oxidation times. There appears to be a larger amount of Au on the tip of the NW than needed for the oxidation reaction. It might be that the Au droplet is constricted by the existing stress in the oxide pillar during the oxidation process.

We observed the phenomenon of enhanced axial oxidation of the NWs in a wet atmosphere at furnace temperatures down to 250 °C. At lower temperatures, e.g. at 100 °C, we could not observe any remarkable oxidation.

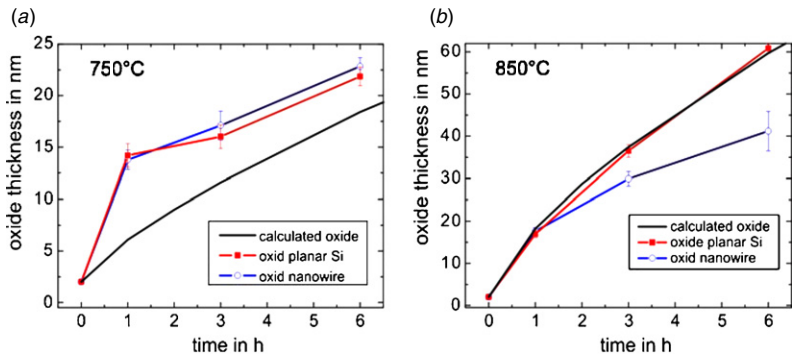

Figure 7. Dry oxidation of ⟨1 1 1⟩ oriented Si NWs in comparison to the oxidation at the planar sites of the same ⟨1 1 1⟩ Si wafer. The thicknesses of SiO_2 layers were generated at (*a*) 750 °C and (*b*) 850 °C, respectively. The thickness is presented as a function of the oxidation time. The curves correspond to (i) experimentally measured data for our planar bulk Si (red), (ii) experiments on Si NWs (blue) and (iii) simulated SiO_2 films, respectively.

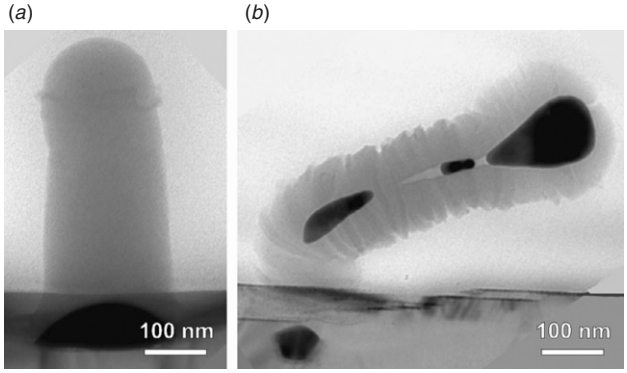

Figure 8. Comparison of the morphology for dry and wet oxidized NWs. (*a*) Dry oxidation at 850 °C, 6 h, (*b*) wet oxidation at 250 °C, 30 min. In both cases, an Au droplet moves down at the reaction interface and reaches the base of the NW after its complete oxidation. Please note that 250 °C is below the eutectic temperature of Au:Si.

4. Conclusion

Au droplets located at the tips of Si NWs play a significant role for the axial enhanced oxidation of ⟨1 1 1⟩ oriented Si NWs. Here we have analyzed the oxidation behavior of MBE-grown NWs. This enhanced oxidation occurs due to the direct contact between the eutectic Au:Si droplet and the Si NW and can be regarded as a negative growth of the Si pillars. The oxidation of dissolved Si atoms at the Au:Si–SiO_2 interface decreases the Si concentration in surface regions inside the droplet resulting in a concentration gradient of dissolved Si atoms toward the Au/Si interface. The bonds of the Si crystal lattice are weakened at the interface by the presence of Au and, thereby, Si atoms can be dissolved in the eutectic droplet. Si diffuses through the droplet and will be oxidized on top of it in an oxidizing atmosphere. This enhanced oxidation is even more severe in a wet atmosphere, where complete oxidation of NWs takes place even at a temperature as low as 250 °C which is below the eutectic temperature of 360 °C for the Au:Si system.

In contrast to the enhanced NW oxidation described, a conventional reaction is observed when there is no direct contact between the Au droplet and the NW. This effect was discovered, e.g., for Si NWs which were stored for 2–3 months in a normal atmosphere. Even a thin oxide layer (thickness 2 nm) between the Si lattice and Au:Si droplet acts as a barrier and the Au atoms cannot weaken the Si lattice bonds.

The described enhanced reaction has to be taken into account for an application of Si NWs as buildings blocks for future electronic devices. Locally restricted acceleration of directional etching (or growing) might have advantages, but also disadvantages. Such an implementation of directional fast etching/oxidation processes by metal particles might be critical for CMOS technology. Related problems can be overcome by a careful metal cleaning process before oxidation or by using other metals. Taking related problems into account, the discussed effect of enhanced oxidation might have a potential application of the nanostructuring of silicon devices.

Acknowledgments

The authors would like to acknowledge the financial support of the European project NODE (contract no. 015783) and the ‘Cluster of Excellence’ of the Land Sachsen-Anhalt.

References

[1] Zhao X, Wei C M, Yang L and Chou M Y 2004 *Phys. Rev. Lett.* **92** 236805
[2] Liu H I, Biegelsen D K, Johnson N M, Ponce F A and Pease R F W 1993 *J. Vac. Sci. Technol.* B **11** 2532
[3] Kederzierski J, Bokor J and Kisielowski C 1997 *J. Vac. Sci. Technol.* B **15** 2825
[4] Büttner C C and Zacharias M 2006 *Appl. Phys. Lett.* **89** 263106
[5] Deal B E and Grove A S 1965 *J. Appl. Phys.* **36** 3770
[6] Massoud H Z and Plummer J D 1985 *J. Electrochem. Soc.* **132** 2693
[7] Kao D B, Mc Vittie J P, Nix W D and Sarawat K C 1987 *IEEE Trans. Electron. Devices* **34** 1008
[8] Kao D B, Mc Vittie J P, Nix W D and Sarawat K C 1988 *IEEE Trans. Electron. Devices* **35** 25

[9] Hiraki A 1984 *Surf. Sci. Rep.* **3** 357
[10] Tu K N 1975 *Appl. Phys. Lett.* **27** 221
[11] Iwami M, Terada T, Tochihara H, Kubota K and Murata Y 1988 *Surf. Sci.* **194** 115
[12] del Giudice M, Joyce J J and Weaver H J 1987 *Phys. Rev.* B **36** 4761
[13] Wagner R S and Ellis W C 1964 *Appl. Phys. Lett.* **4** 89
[14] Schubert L, Werner P, Zakharov N D, Gerth G, Kolb F M, Long L and Gösele U 2004 *Appl. Phys. Lett.* **84** 4968
[15] Zakharov N, Werner P, Sokolov L and Gösele U 2007 *Physica* E **37** 148
[16] Westwater J, Gosain D P, Tomiya S, Hirano Y and Usui S 1997 *Mater. Res. Soc. Symp. Proc.* **452** 237
[17] Werner P, Büttner C, Schubert L, Gerth G, Zakharov N D and Gösele U 2007 *Int. J. Mater. Res.* **98** 1066
[18] Werner P, Zakharov N D, Gerth G, Schubert L and Gösele U 2006 *Int. J. Mater. Res.* **97** 1008
[19] Okamoto H and Massalski T B 1990 *Binary Alloy Phase Diagrams* vol 1 (Materials Park, OH: ASM International)
[20] Ghandhi S K 1994 *VLSI Fabrication Principles Silicon and Gallium Arsenide* 2nd edition (New York: Wiley)
[21] Xie T, Schmidt V, Pippel E, Senz S and Gösele U 2007 *Small* **4** 64